Jundishapur J Microbiol. 2016 May; 9(5):e29773. doi: 10.5812/jjm.29773.

Published online 2016 February 15. **Research Article**

Comparison of Newly Assembled Full Length HIV-1 Integrase With Prototype Foamy Virus Integrase: Structure-Function Prospective

Mohammad Reza Dayer[1,*]

[1]Department of Biology, Faculty of Science, Shahid Chamran University, Ahvaz, IR Iran

[*]*Corresponding author*: Mohammad Reza Dayer, Department of Biology, Faculty of Sciences, Shahid Chamran University, Ahvaz, IR Iran. Tel: +98-6113331045, Fax: +98-6113331045, E-mail: mrdayer@scu.ac.ir

Received 2015 May 09; **Revised** 2015 November 17; **Accepted** 2015 November 30.

Abstract

Background: Drug design against human immunodeficiency virus type 1 (HIV-1) integrase through its mechanistic study is of great interest in the area in biological research. The main obstacle in this area is the absence of the full-length crystal structure for HIV-1 integrase to be used as a model. A complete structure, similar to HIV-1 of a prototype foamy virus integrase in complex with DNA, including all conservative residues, is available and has been extensively used in recent investigations.
Objectives: The aim of this study was to determine whether the above model is precisely representative of HIV-1 integrase. This would critically determine the success of any designed drug using the model in deactivation of integrase and AIDS treatment.
Materials and Methods: Primarily, a new structure for HIV-1 was constructed, using a crystal structure of prototype foamy virus as the starting structure. The constructed structure of HIV-1 integrase was simultaneously simulated with a prototype foamy virus integrase on a separate occasion.
Results: Our results indicate that the HIV-1 system behaves differently from the prototype foamy virus in terms of folding, hydration, hydrophobicity of binding site and stability.
Conclusions: Based on our findings, we can conclude that HIV-1 integrase is vastly different from the prototype foamy virus integrase and does not resemble it, and the modeling output of the prototype foamy virus simulations could not be simply generalized to HIV-1 integrase. Therefore, our HIV-1 model seems to be more representative and more useful for future research.

Keywords: Human Immunodeficiency Virus Type-1, Integrase, Prototype Foamy Virus, Molecular Dynamic Simulation

1. Background

The human immunodeficiency virus type 1 (HIV-1) integrase EC 2.7.7.49 is a key enzyme responsible for integration of viral DNA into the host cell DNA; the process that is mandatory for viral replication and host cell infection (1-3). Unlike protease and reverse transcriptase of HIV-1 virus, integrase has no analogue in host cells; therefore, viral infection is highly dependent on integrase activity. Accordingly, integrase deactivation could be considered as an effective way for acquired immune deficiency syndrome (AIDS) treatment (4-9).

Integrase is a single stranded 32 kDa protein with 288 residues encoded by the 3' end of the POL gene. The structural analysis of integrase protein revealed that it has three distinct domains, each with specific functions (10, 11) These domains include the N-terminal domain (NTD), residues 1 - 50, with zinc binding motif of HHCC that takes part in enzyme multimerization i.e. formation of functional multimeric assemblies as tetramers or octamers (12-14); and the catalytic core domain (CCD), residues 51 - 212, that contains a conservative catalytic motif of DD35E, which is composed of Asp^{64}, Asp^{116} and Glu^{152}. This domain with the aid of two magnesium ions (Mg^{+2}) catalyzes the integration of viral DNA into host cell genome. The first magnesium ion is placed between Asp^{128} and Asp^{185} (A-site) and the next magnesium ion is placed between Asp^{128} and Glu^{221} (B-site).

The magnesium ion of the B-site makes a pentahedral complex with the two carboxyl groups of Asp^{128} and Glu^{221}, hydroxyl group of 3'-OH of dA nucleotide and two H_2O molecules. This complex activates the 3'-OH group for a nucleophilic attack on host cell DNA. In this context, the A-site stabilizes the pentahedral complex of the B-site and guarantees the integration process. Moreover, it has been shown that the CCD domain facilitates DNA binding to the enzyme binding site (15, 16). The last domain of integrase, residues 213 - 288, is called the C-terminal domain (CTD), which is believed to act as a non specific binding site for DNA (12, 14, 17-19).

The integration catalyzed by integrase could be divided into two distinct processes. The first process is called 3'-OH processing, in which integrase in the host cell cytoplasm binds to the CAGT sequence at both ends of the viral DNA, hydrolyzes G and T nucleotides and leaves the naked

3'-OH on the last nucleotides (20, 21). The next process is called the strand transfer process, in which integrase in host cell nucleus uses Mg^{2+}-activated 3'-OH groups of B-site to attack host cell DNA to integrate viral DNA (22, 23).

Based on this mechanism, there are two classes of inhibitors designed against these two processes: 1-inhibitors against the 3'-OH process at the DNA binding site, known as integrase binding inhibitors (IBIN) and 2-inhibitors against the integrase-DNA (or pre-integration) complex. These inhibitors, which bind to Mg^{2+} ions of the binding site and prevent DNA transfer to the host cell genome, are called integrase strand transfer inhibitors (INSTI) (24-28).

Even though the full-length crystal structure of integrase from prototype foamy virus (PFV) in complex with DNA is available to model HIV-1 integrase in bioinformatics methods for drug design, there is an essential need for the full-length coordinate structure of HIV-1 integrase (29-39).

2. Objectives

In the present work, we attempted to construct a full-length coordinate structure for HIV-1 integrase using the PFV integrase as the starting structure in a bid to obtain more effective drugs. Finally, we decided to simulate, in parallel experiments, the new HIV-1 integrase and an intact copy of PFV integrase to compare them, from a structural point of view, to see whether the two structures show similar dynamic behaviors. This, presumably, helps identify which of the structures is more representative of viral HIV-1 integrase.

3. Materials and Methods

3.1. Crystal Structures Used

The crystal structure of wild type PFV in the protein data bank (PDB) (ID number 3L2T) with no mutation, was used as a native structure for PFV throughout this study. The structure, which was obtained by the X-ray diffraction method and refined at the resolutions of 2.0 Å, was retrieved from the protein data bank (http://www.rcsb.org/pdb) (40).

3.2. Sequence Alignment

The sequence of wild type HIV-1 integrase in FASTA format was obtained from http://www.bioafrica.net/ as presented in Figure 1. This sequence was then aligned with the PFV sequence on the http://fasta.bioch.virginia.edu/ server to match their sequence similarity (Figure 1 B).

3.3. Constructing a New Structure for HIV-1 Integrase

To construct a coordinate structure for HIV-1 integrase based on the PFV structure, we used a copy of the 3L2T.PDB file and renamed it HIV-1.pdb. This file was opened in the text editor software and 59 residues from the N-terminal and 15 residues from the C-terminal were deleted to provide a protein with appropriate length for HIV-1 integrase. The file was then opened in the Swiss-Pdb Viewer software (http://www.expasy.org/) and the residues were mutated according to alignment results presented in Figure 1 B to match the HIV-1 integrase sequence (41, 42). In this process, the constructed structure was energy-minimized.

3.4. Systems Preparation

The final constructed structure for HIV-1 was placed in the center of a rectangular box with the following dimensions, $8.15 \times 9.06 \times 9.58$ nm, for further experimentation. An intact copy of 3L2T.pdb was used as an intact PFV integrase and placed in the same box with $9.44 \times 9.26 \times 10.63$ nm dimensions. The two boxes were then filled with SPCE solvents using the genbox command of GROMACS package so that the proteins were covered by a water shell of 1.0-nm thickness.

3.5. Molecular Dynamic (MD) Simulation

The experiments were performed using the double-precision MPI version of GROMACS 4.5.5 installed on the UBUNTU version 12.10 with amber 99sb force field (43). The net charges of simulated systems were analyzed by the preprocessor engine of the GROMACS package. System neutralization was done by adding equivalent numbers of positive sodium ions. Energy minimization was performed for hydrogen atoms, ions and solvents in 1500 steps, using the steepest descent method to minimize the system energy to at least 300 kJ/mol. Linear constraint solver (LINCS) algorithm was used to apply constraint on bonds lengths. The SETTLE algorithm was also used to constrain the geometry of solvents.

The systems were then subjected to a short molecular dynamic with all-bonds restrains for a period of 500 ps, before performing a full MD without any restrains (44). All simulations were carried out for 10 ns at 37°C and one atmospheric pressure. Berendsen, and Thermostat and Barostat, were used for temperature and pressure coupling, respectively and the Particle Mesh Ewald (PME) method for electrostatic interactions. The time steps of one femtosecond were applied to all simulations. All of these simulations were done at neutral pH (Asp, Glu, Arg and Lys ionized) (45, 46).

Figure 1. The Sequence of Wild Type HIV-1 Integrase in FASTA Format

A

```
HIV-1 (HXB2):

        10         20         30         40         50         60         70
         |          |          |          |          |          |          |
FLDGIDKAQD EHEKYHSNWR AMASDFNLPP VVAKEIVASC DKCQLKGEAM HGQVDCSPGI WQLDCTHLEG

        80         90         100        110        120        130        140
         |          |          |          |          |          |          |
KVILVAVHVA SGYIEAEVIP AETGQETAYF LLKLAGRWPV KTIHTDNGSN FTGATVRAAC WWAGIKQEFG

        150        160        170        180        190        200        210
         |          |          |          |          |          |          |
IPYNPQSQGV VESMNKELKK IIGQVRDQAE HLKTAVQMAV FIHNFKRKGG IGGYSAGERI VDIIATDIQT

        220        230        240        250        260        270        280
         |          |          |          |          |          |          |
KELQKQITKI QNFRVYYRDS RNPLWKGPAK LLWKGEGAVV IQDNSDIKVV PRRKAKIIRD YGKQMAGDDC

     288
```

B

```
           40        50        60        70        80        90        100       110
HIV-1   AKEIVASCDKCQLKGEAMHGQVDCSPGIWQLDCTHLEGKVILVAVHVASGYIEAEVIPAETGQETAYFLLKLAGRWPVKT
                                                .::.:   .:.       : . . :.  :  :..    :.
PFV     TNASNKASGPILRPDRPQKPFDKFFIDYIGPLPPSQGYLYVLVVVDGMTGFTWLYPTKAPSTSATVKSLNVLTSIAIPKV
           110       120       130       140       150       160       170       180

           120       130       140       150       160       170       180       190
HIV-1   IHTDNGSNFTGATVRAACWWA--GIKQEFGIPYNPQSQGVVESMNKELKKIIGQVRDQAEHLKTAVQMAVFIHNFKRKGG
        ::.:.:. ::..:   : :    ::. ::. ::.:::.: ::  :...:... ..
PFV     IHSDQGAAFTSSTF--AEWAKERGIHLEFSTPYHPQSSGKVERKNSDIKRLLTKLLVGRPTKWYDLLPVVQLALNNTYSP
           190       200       210       220       230       240       250       260

           200       210       220       230       240       250       260       270
HIV-1   IGGYSAGERIVDIIATDIQTKELQKQITKIQNFRVYYRDSRNPLWKGPAKLLWKGEGAVVIQDNSDIKVVPRRKAKIIRD

PFV     VLKYTPHQLLFGIDSNTPFANQDTLDLTREEELSLLQEIRTSLYHPSTPPASSRSWSPVVGQLVQERVARPASLRPRWHK
           270       280       290       300       310       320       330       340
```

A, Wild-type HIV-1 integrase sequence in FASTA format obtained from the http://www.bioafrica.net/ website; B, sequence alignment results for wild-type HIV-1 and PFV integrase obtained from the http://fasta.bioch.virginia.edu/ Server.

3.6. Docking Experiments

Binding energy of DNA to each integrase was calculated using the Hex software version 5.1 (http://www.loria.fr/) (47). The default-shape only mode of correlation was used to study the physical fitness of DNA to their binding site in HIV-1 and PFV integrase. Docking results were scored based on their energy and the first 100 solutions were averaged to obtain the binding energy of DNA to integrase.

The Argus-Lab 4.0.1 Software (http://www.arguslab.com) was used to extract binding site residues that participate in DNA binding to integrase (48).

4. Results

As indicated in Figure 2 A, HIV-1 undergoes more structural alterations than PFV upon simulation with a greater increase in the Root Mean Square Displacement (RMSD) curve. This means that HIV-1 integrase experiences extensive changes in its tertiary structure while attaining its equilibrated structure at about 3000 ps. On the other hand, in equilibrated states, at 5000 - 10000 ps, the RMSD curve of PFV shows more variation than that of HIV-1 integrase. The less fluctuating RMSD is an indication of a more stable and less flexible structure for the HIV-1 integrase. Figure 2 indicates that DNA- HIV-1 integrase complex is tighter and less flexible.

Figures 3 A and B show root mean square fluctuation

Figure 2. Root Mean Square Displacement

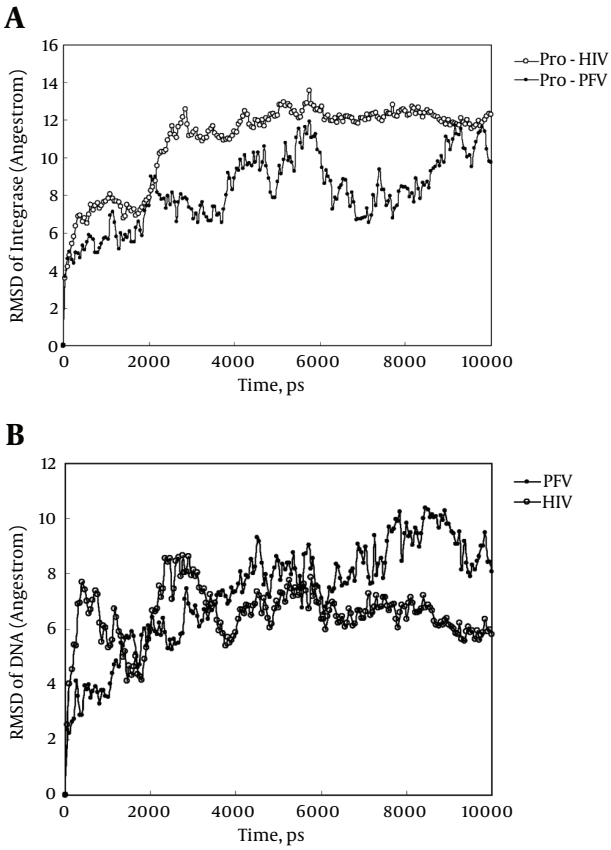

A, Root mean square displacement plot of HIV-1 and prototype foamy virus integrase backbone against their initial state obtained at 37°C and one atmospheric pressure in SPCE water box; B, root mean square displacement plot of DNA of HIV-1 and prototype foamy virus integrase-DNA complex against their initial state obtained at 37°C and one atmospheric pressure in SPCE water box and shows the RMSD progression of complexes of DNA with HIV-1 and PFV in comparison to their initial state.

(RMSF) plots for alpha carbons of HIV-1 and PFV during simulation, respectively. As depicted, the RMSF of each domain of N-terminal domain (NTD), catalytic core domain (CCD) and C-terminal domain (CTD) from HIV-1 (Figure 2 A) could be compared to their counterparts on the PFV system, separately (Figure 2 B). These drawing show that CCD domains of both systems in contrast to NTD and CTD domains, show lower RMSF values and lower flexibilities during simulation.

Figure 3 C illustrates the average RMSF values for HIV-1 and PFV CCD domain. Higher values of RMSF for PFV ($P < 0.001$) may be attributed to its longer domains of NTD and CTD with extra 59 and 15 residues, respectively, in contrast to HIV-1 integrase. Longer flexible tails of PFV provide a source for more flexibility and instability in its tertiary structure and leads to a loosely folded conformation.

Figure 3. show Root Mean Square Fluctuation (RMSF)

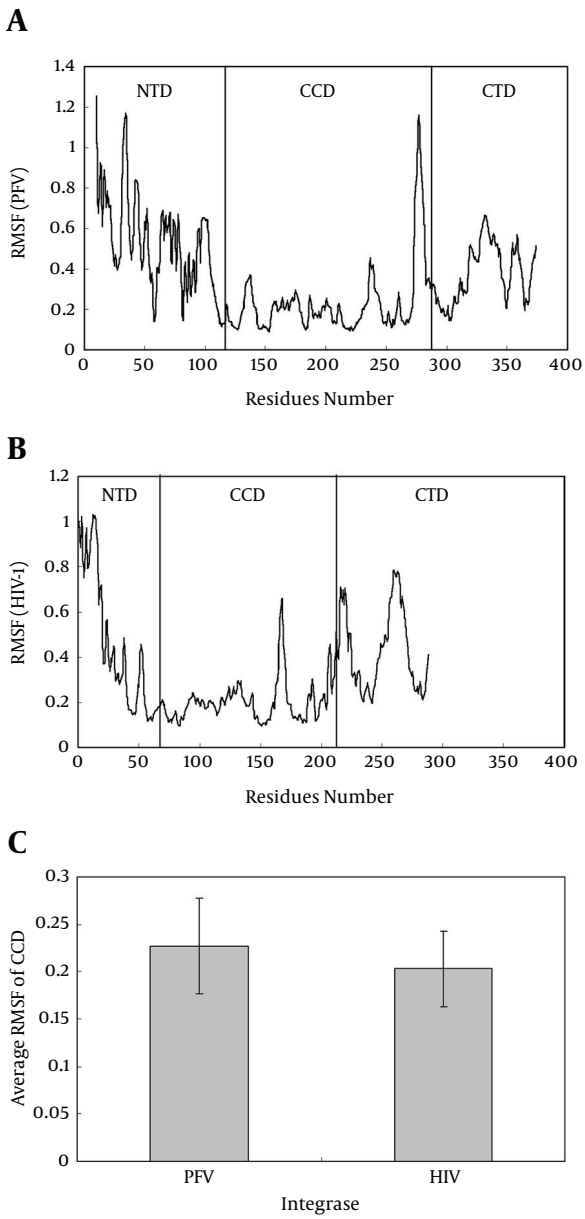

A, Root mean square displacement plot of prototype foamy virus integrase obtained for 10 ns Simulation at 37°C and one atmospheric pressure in SPCE water box; B, root mean square displacement Plot of HIV-1 Integrase Obtained for 10 ns simulation at 37°C and one atmospheric pressure in SPCE water box; C, average root mean square displacement for catalytic residues of prototype foamy virus (Residues 120 - 282) and HIV-1 (Residues 50 - 212) calculated from data of Figure 4 A and B as average ± SD ($P < 0.05$)

The MSD curve of DNA displacement inside integrase during simulation showed more tightly bound DNA to HIV-1 with retained propagation in contrast to PFV integrase (data not shown). In other word, the Figure 3 indicates that

DNA was held more strongly by HIV-1 integrase via its binding site than by PFV integrase.

The first hydration layer of macromolecules is described as a dense layer of solvents arranged at a distance of 3 - 5 angstroms from the macromolecule backbone. This layer plays an important role in structure-function cooperation of macromolecules. To show the difference of thickness in the hydration layer of HIV-1 and PFV, we calculated the first hydration layers for both simulated systems. These calculations (data not shown) indicated that the population of solvents in the first hydration layer of PFV was two times more than that of HIV-1 integrase. These findings, being in accordance with our results, confirm that PFV integrase has a more extended structure with more extended hydration layer compared to HIV-1. The data was interpreted as a more extended structure for PFV-DNA complex with a loosely folded structure in contrast to HIV-1-DNA complex.

Figure 4 shows the hydrophobic part of accessible solvent area (ASA) for HIV-1 and PFV integrases during simulation periods. Since HIV-1 integrase structure used in this experiment does not equilibrate before simulation, it is expected to express higher ASA during the early phase of simulation (Figure 4). Progress in ASA for HIV-1, gradually pushes integrase toward its native state with decreased ASA. Ultimately, HIV-1 integrase reaches its equilibrated structure with similar ASA as PFV.

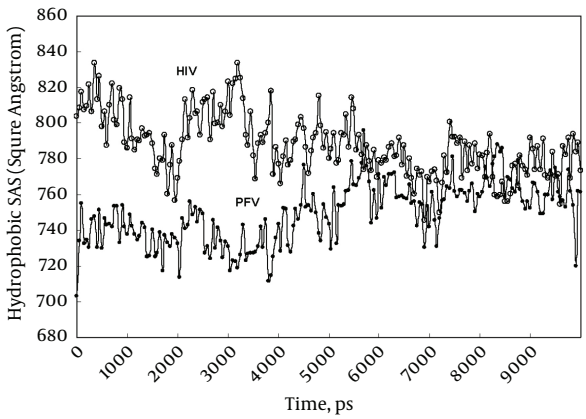

Figure 4. Hydrophobic Accessible Area (ASA) Curve of HIV-1 and Prototype Foamy Virus Integrase Changes During 10 ns Period of Simulation at 37°C and One Atmospheric Pressure, in the Presence of SPCE Water Box

Intra-molecular hydrogen bonds include bonds formed between secondary or tertiary structure elements. Time course determination of these hydrogen bonds for our simulated systems provide valuable information about our systems.

Given that the counts of bonds are proportional to residue numbers, we calculated the intra-molecular bonds formed per residue to make a reasonable comparison between HIV-1 integrase and PFV. We found that about 1.8 and 1.5 hydrogen bonds formed per residue in HIV-1 integrase and PFV integrase, respectively. This finding indicates that the more hydrogen bonds are formed, the more stable conformation for HIV-1 integrase will be.

Binding site hydrophobicity of integrase for DNA is another useful index to structurally compare HIV-1 with PFV. Hydrophobicity could be calculated for a binding site by summation of hydrophobic indices of residues comprising of enzyme active site. In order to calculate hydrophobicity, we first extracted residues of active site for each integrase by the Argus-Lab 4.0.1 software (http://www.arguslab.com). Our data showed that PFV binding site includes residues Asp^{128}, Tyr^{129}, Asp^{185}, Phe^{190}, Tyr^{212}, His^{213}, Pro^{214}, Gln^{215}, Glu^{221}, Asn^{224} and Arg^{326}, and HIV-1 binding site includes Ile^{60}, Trp^{61}, Gln^{62}, Leu^{63}, Asp^{64}, Asp^{116}, Phe^{121}, Gln^{148}, Glu^{152}, Asn^{155} and Lys^{159}. Then, using the Kyte-Doolittle scale for hydrophobicity, we calculated the total hydrophobic index for active site residues of HIV-1 and PFV. The total hydrophobic index of HIV-1 and PFV were calculated as -14.7 and -28.3, respectively (48). The more hydrophobic index for HIV-1 integrase (more positive) indicates its stronger hydrophobicity compared to PFV, which means that DNA makes a more stable complex with HIV-1 than PFV.

This finding encouraged us to calculate the direct binding energy of DNA to both integrase, HIV-1 and PFV, by performing docking experiments. Using the Hex software version 5.1 (http://www.loria.fr/), we performed docking experiments for DNA with both HIV-1 and PFV. Our results indicate that the binding energy of DNA to HIV-1 integrase and to PFV integrase are-662 KJ/Mol and -658 KJ/Mol, respectively. The higher binding energy of DNA to HIV-1 (about 14 KJ/mol higher) confirmed again the higher stability of DNA-HIV-1 complex compared to DNA-PFV complex.

Structural survey of HIV-1 and PFV integrase active sites and their changes during simulation reveals very interesting facts regarding different arrangements of active site residues around the 3'-dA nucleotide and magnesium ions at B-sites. Figure 5 A shows the arrangement of active site residues of HIV-1 integrase around 3'-dA and Mg^{2+} ion before (left) and after (right) simulation. Figure 5 shows that 3'-dA and Mg^{2+} are inserted into a binding cleft during simulation to a place far from the accessibility of foreign ligands such as enzyme inhibitors.

Figure 5 B shows the same change in PFV integrase. As shown, in the case of PFV integrase, dA and Mg^{2+} did not enter in the same active site cleft as in the case of HIV-1 integrase. We, therefore, hypothesized that the chelation of B-site magnesium ion by 3'-processing inhibitors is more

Figure 5. Graphic Representation of DNA Binding Site

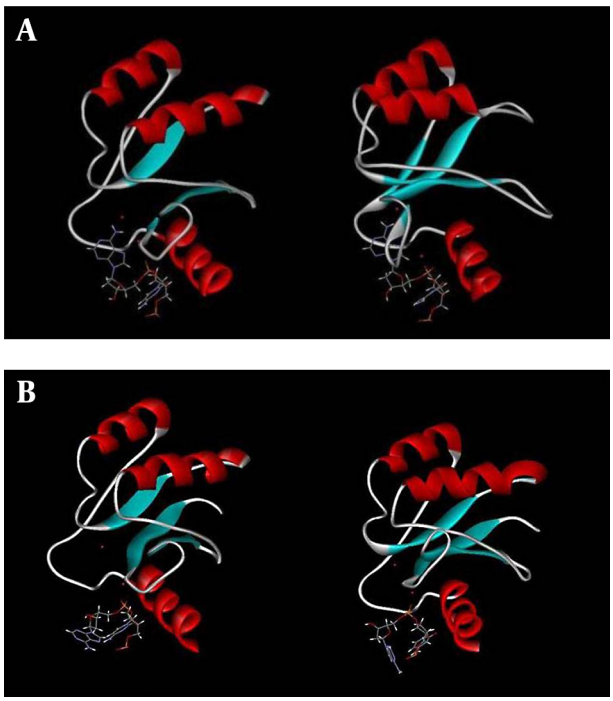

A, Graphic representation of DNA binding site of HIV-1 integrase before (left) and after (right) simulation showing the movement of the 3'-dA through the binding site cleft obtained from 10 ns simulation at 37°C and one atmospheric pressure, in the presence of SPCE water box; B, Graphic representation of DNA binding site of PFV integrase before (left) and after (right) simulation showing the situation of 3'-dA and magnesium ions of A and B sites obtained from 10 ns simulation at 37°C and one atmospheric pressure, in the presence of SPCE water box.

difficult in HIV-1 than in PFV integrase. In other words, the PFV binding site seems to be more extended and its magnesium ions are more accessible to enzyme inhibitors attack compared to HIV-1.

5. Discussion

It is well known that there is two types of integrase inhibitors used in chemotherapy of HIV-1 infected patients. The first type (IBIN) attacks DNA binding site on the integrase, binds magnesium ions and prevents viral DNA to bind and interact with the 3'-OH group. In most cases, this inhibitor fails because viral DNA binds to integrase prior to drug therapy and there is no free enzyme to be attacked by inhibitors.

The second type of inhibitor (INSTI) binds to magnesium ions and stacks to penultimate nucleotide of cytidine, pushes the last nucleotide of adenosine and its 3'-OH group outside the enzyme binding site and prevents integrase to recruit 3'-OH to attack host cell DNA. Our findings show wide structural differences between HIV-1 and PFV integrases, which make them behave differently against inhibitors.

Figure 2 A and B indicate that the equilibrated structure of HIV-1 integrase has a more stable structure with lower RMSD than PFV. Figure 3 A - C emphasize the more stable structure of HIV-1 integrase with lower RMSF especially at the CCD domain. Our data also indicate a more hydrophobic binding site for HIV-1 integrase with stronger binding capacity to viral DNA. Measurements of direct binding energy of DNA to integrase systems confirm our findings about higher HIV-1 affinity for DNA binding (~ 14 KJ/Mol higher). Finally, Figure 5 A and B precisely show the difference between the active site configuration around 3'-dA and Mg^{2+} of HIV-1 and PFV integrase. The active site configuration of HIV-1 hides the Mg^{2+} ion of the B-site to be away from the reach of inhibitors. We hypothesized that this is the main cause for higher resistance of HIV-1 against metal chelating inhibitors.

Based on our findings, we can conclude that viral DNA-PFV integrase complex that is widely used in recent studies as a representative model for HIV-1 integrase does not seem to be a reliable model for drug design against AIDS. Hence, we recommend that relevant reports should be rechecked using more realistic models as the one we constructed.

Acknowledgments

The author would like to express his thanks to the vice chancellor of research and technology of Shahid Chamran university of Ahvaz for their financial support.

Footnote

Funding/Support: This research was financially supported by grant No. 94302424: department of research affairs of Shahid Chamran university of Ahvaz, Ahvaz, Iran.

References

1. Xue W, Jin X, Ning L, Wang M, Liu H, Yao X. Exploring the molecular mechanism of cross-resistance to HIV-1 integrase strand transfer inhibitors by molecular dynamics simulation and residue interaction network analysis. *J Chem Inf Model.* 2013;**53**(1):210–22. doi: 10.1021/ci300541c. [PubMed: 23231029].
2. Feller L, Khammissa RAG., Wood NH, Meyerov R, Lemmer J. Insights into immunopathogenic mechanisms of HIV infection: high levels of immune activation and HIV fitness: communication corner. *South African Dental Journal.* 2008;**63**(10):552–7.
3. Hammer SM, Saag MS, Schechter M, Montaner JSG, Schooley RT, Jacobsen DM, et al. Treatment for Adult HIV Infection. *Jama.* 2006;**296**(7):827. doi: 10.1001/jama.296.7.827.

4. Pommier Y, Johnson AA, Marchand C. Integrase inhibitors to treat HIV/AIDS. *Nat Rev Drug Discov.* 2005;**4**(3):236–48. doi: 10.1038/nrd1660. [PubMed: 15729361].
5. Savarino A. A historical sketch of the discovery and development of HIV-1 integrase inhibitors. *Expert Opin Investig Drugs.* 2006;**15**(12):1507–22. doi: 10.1517/13543784.15.12.1507. [PubMed: 17107277].
6. DeJesus E, Berger D, Markowitz M, Cohen C, Hawkins T, Ruane P, et al. Antiviral activity, pharmacokinetics, and dose response of the HIV-1 integrase inhibitor GS-9137 (JTK-303) in treatment-naive and treatment-experienced patients. *J Acquir Immune Defic Syndr.* 2006;**43**(1):1–5. doi: 10.1097/01.qai.0000233308.82860.2f. [PubMed: 16936557].
7. Markowitz M, Morales-Ramirez JO, Nguyen BY, Kovacs CM, Steigbigel RT, Cooper DA, et al. Antiretroviral activity, pharmacokinetics, and tolerability of MK-0518, a novel inhibitor of HIV-1 integrase, dosed as monotherapy for 10 days in treatment-naive HIV-1-infected individuals. *J Acquir Immune Defic Syndr.* 2006;**43**(5):509–15. doi: 10.1097/QAI.0b013e31802b4956. [PubMed: 17133211].
8. Johnson BC, Metifiot M, Pommier Y, Hughes SH. Molecular dynamics approaches estimate the binding energy of HIV-1 integrase inhibitors and correlate with in vitro activity. *Antimicrob Agents Chemother.* 2012;**56**(1):411–9. doi: 10.1128/AAC.05292-11. [PubMed: 22037850].
9. Nowotny M. Retroviral integrase superfamily: the structural perspective. *EMBO Rep.* 2009;**10**(2):144–51. doi: 10.1038/embor.2008.256. [PubMed: 19165139].
10. Rice PAP, Baker TA. Comparative architecture of transposase and integrase complexes. *Nat Struct Mol Biol.* 2001;**8**(4):302–7. [PubMed: 11276247].
11. Chen X, Tsiang M, Yu F, Hung M, Jones GS, Zeynalzadegan A, et al. Modeling, analysis, and validation of a novel HIV integrase structure provide insights into the binding modes of potent integrase inhibitors. *J Mol Biol.* 2008;**380**(3):504–19. doi: 10.1016/j.jmb.2008.04.054. [PubMed: 18565342].
12. Jayappa KD, Ao Z, Yang M, Wang J, Yao X. Identification of critical motifs within HIV-1 integrase required for importin alpha3 interaction and viral cDNA nuclear import. *J Mol Biol.* 2011;**410**(5):847–62. doi: 10.1016/j.jmb.2011.04.011. [PubMed: 21763491].
13. Agapkina J, Smolov M, Barbe S, Zubin E, Zatsepin T, Deprez E, et al. Probing of HIV-1 integrase/DNA interactions using novel analogs of viral DNA. *J Biol Chem.* 2006;**281**(17):11530–40. doi: 10.1074/jbc.M512271200. [PubMed: 16500899].
14. Grobler JA, Stillmock K, Hu B, Witmer M, Felock P, Espeseth AS, et al. Diketo acid inhibitor mechanism and HIV-1 integrase: implications for metal binding in the active site of phosphotransferase enzymes. *Proc Natl Acad Sci.* 2002;**99**(10):6661–6. [PubMed: 11997448].
15. Marchand C, Johnson AA, Karki RG, Pais GCG, Zhang X, Cowansage K, et al. Metal-dependent inhibition of HIV-1 integrase by β-diketo acids and resistance of the soluble double-mutant (F185K/C280S). *Mol Pharmacol.* 2003;**64**(3):600–9. [PubMed: 12920196].
16. Chen JCH, Krucinski J, Miercke LJW, Finer-Moore JS, Tang AH, Leavitt AD, et al. Crystal structure of the HIV-1 integrase catalytic core and C-terminal domains: a model for viral DNA binding. *Proc Natl Acad Sci.* 2000;**97**(15):8233–8. [PubMed: 10890912].
17. Craigie R. HIV integrase, a brief overview from chemistry to therapeutics. *J Biol Chem.* 2001;**276**(26):23213–6. doi: 10.1074/jbc.R100027200. [PubMed: 11346660].
18. Nomura Y, Masuda T, Kawai G. Structural analysis of a mutant of the HIV-1 integrase zinc finger domain that forms a single conformation. *J Biochem.* 2006;**139**(4):753–9. doi: 10.1093/jb/mvj085. [PubMed: 16672276].
19. Almerico A, Tutone M, Ippolito M, Lauria A. Molecular Modelling and QSAR in the Discovery of HIV-1 Integrase Inhibitors. *Curr Comput Aided Drug Des.* 2007;**3**(3):214–33. doi: 10.2174/157340907781695468.
20. Dicker IB, Samanta HK, Li Z, Hong Y, Tian Y, Banville J, et al. Changes to the HIV long terminal repeat and to HIV integrase differentially impact HIV integrase assembly, activity, and the binding of strand transfer inhibitors. *J Biol Chem.* 2007;**282**(43):31186–96. doi: 10.1074/jbc.M704935200. [PubMed: 17715137].
21. Huang M, Grant GH, Richards WG. Binding modes of diketo-acid inhibitors of HIV-1 integrase: a comparative molecular dynamics simulation study. *J Mol Graph Model.* 2011;**29**(7):956–64. doi: 10.1016/j.jmgm.2011.04.002. [PubMed: 21531158].
22. Pommier Y, Marchand C, Neamati N. Retroviral integrase inhibitors year 2000: update and perspectives. *Antiviral Research.* 2000;**47**(3):139–48. doi: 10.1016/s0166-3542(00)00112-1.
23. Metifiot M, Marchand C, Maddali K, Pommier Y. Resistance to integrase inhibitors. *Viruses.* 2010;**2**(7):1347–66. [PubMed: 20706558].
24. Hazuda DJ, Felock P, Witmer M, Wolfe A, Stillmock K, Grobler JA, et al. Inhibitors of strand transfer that prevent integration and inhibit HIV-1 replication in cells. *Science.* 2000;**287**(5453):646–50. [PubMed: 10649997].
25. Zhuang L, Wai JS, Embrey MW, Fisher TE, Egbertson MS, Payne LS, et al. Design and synthesis of 8-hydroxy-[1,6]naphthyridines as novel inhibitors of HIV-1 integrase in vitro and in infected cells. *J Med Chem.* 2003;**46**(4):453–6. doi: 10.1021/jm025553u. [PubMed: 12570367].
26. Marchand C, Zhang X, Pais GC, Cowansage K, Neamati N, BurkeTR Jr., et al. Structural determinants for HIV-1 integrase inhibition by beta-diketo acids. *J Biol Chem.* 2002;**277**(15):12596–603. doi: 10.1074/jbc.M110758200. [PubMed: 11805103].
27. Zouhiri F, Mouscadet JF, Mekouar K, Desmaele D, Savoure D, Leh H, et al. Structure-activity relationships and binding mode of styrylquinolines as potent inhibitors of HIV-1 integrase and replication of HIV-1 in cell culture. *J Med Chem.* 2000;**43**(8):1533–40. [PubMed: 10780910].
28. Chen JCH, Krucinski J, Miercke LJW, Finer-Moore JS, Tang AH, Leavitt AD, et al. Crystal structure of the HIV-1 integrase catalytic core and C-terminal domains: a model for viral DNA binding. *Proc Acad Sci.* 2000;**97**(15):8233–8. [PubMed: 10890912].
29. Cherepanov P, Ambrosio ALB, Rahman S, Ellenberger T, Engelman A. Structural basis for the recognition between HIV-1 integrase and transcriptional coactivator p75. *Proc Natl Acad Sci.* 2005;**102**(48):17308–13. [PubMed: 16260736].
30. Yuan P, Gupta K, Van Duyne GD. Tetrameric structure of a serine integrase catalytic domain. *Structure.* 2008;**16**(8):1275–86. doi: 10.1016/j.str.2008.04.018.
31. Goldgur Y, Craigie R, Cohen GH, Fujiwara T, Yoshinaga T, Fujishita T, et al. Structure of the HIV-1 integrase catalytic domain complexed with an inhibitor: a platform for antiviral drug design. *Proc Natl Acad Sci.* 1999;**96**(23):13040–3. [PubMed: 10557269].
32. Wielens J, Headey SJ, Jeevarajah D, Rhodes DI, Deadman J, Chalmers DK, et al. Crystal structure of the HIV-1 integrase core domain in complex with sucrose reveals details of an allosteric inhibitory binding site. *FEBS Lett.* 2010;**584**(8):1455–62. doi: 10.1016/j.febslet.2010.03.016. [PubMed: 20227411].
33. Wang JY, Ling H, Yang W, Craigie R. Structure of a two-domain fragment of HIV-1 integrase: implications for domain organization in the intact protein. *EMBO J.* 2001;**20**(24):7333–43. doi: 10.1093/emboj/20.24.7333. [PubMed: 11743009].
34. Cherepanov P, Sun ZY, Rahman S, Maertens GN, Wagner G, Engelman A. Solution structure of the HIV-1 integrase-binding domain in LEDGF/p75. *Nat.Struct Mol Biol.* 2005;**12**(6):526–32. [PubMed: 15895093].
35. Me´tifiot M, Maddali K, Johnson BC, Hare S, Smith SJ, Zhao XZ, et al. Activities, crystal structures, and molecular dynamics of dihydro-1 H-isoindole derivatives, inhibitors of HIV-1 integrase. *ACS chemical biology.* 2012;**8**(1):209–17. doi: 10.1021/cb300471n.
36. Hare S, Gupta S, Valkov E, Engelman A, Cherepanov P. Retroviral intasome assembly and inhibition of DNA strand transfer. *Nature.* 2010;**464**(7286):232–6. doi: 10.1038/nature08784.
37. Maertens GN, Hare S, Cherepanov P. The mechanism of retroviral integration from X-ray structures of its key intermediates. *Nature.* 2010;**468**(7321):326–9. doi: 10.1038/nature09517.
38. Hare S, Vos AM, Clayton RF, Thuring JW, Cummings MD, Cherepanov

P. Molecular mechanisms of retroviral integrase inhibition and the evolution of viral resistance. *Nat Struct Mol Biol.* 2010;**107**(46):20057–62. doi: 10.1073/pnas.1010246107.
39. Stiffin RM, Sullivan SM, Carlson GM, Holyoak T. Differential inhibition of cytosolic PEPCK by substrate analogues. Kinetic and structural characterization of inhibitor recognition. *Biochemistry.* 2008;**47**(7):2099–109. doi: 10.1021/bi7020662. [PubMed: 18197707].
40. Guex N, Peitsch MC. SWISS-MODEL and the Swiss-PdbViewer: an environment for comparative protein modeling. *Electrophoresis.* 1997;**18**(15):2714–23. doi: 10.1002/elps.1150181505. [PubMed: 9504803].
41. Johnson VA, Brun-Vezinet F, Clotet B, Gunthard HF, Kuritzkes DR, Pillay D, et al. Update of the drug resistance mutations in HIV-1: Spring 2008. *Top HIV Med.* 2008;**16**(1):62–8.
42. Dayer MR, Dayer MS. Whiskers-less HIV-protease: a possible way for HIV-1 deactivation. *J Biomed Sci.* 2013;**20**:67. doi: 10.1186/1423-0127-20-67. [PubMed: 18441382].
43. Kirk W, Kurian E, Wessels W. Photophysics of ANS. V. Decay modes of ANS in proteins: the IFABP-ANS complex. *Biophys Chem.* 2007;**125**(1):50–8. doi: 10.1016/j.bpc.2006.07.020. [PubMed: 16979813].
44. Konkle ME, Muellner SK, Schwander AL, Dicus MM, Pokhrel R, Britt RD, et al. Effects of pH on the Rieske protein from Thermus thermophilus: a spectroscopic and structural analysis. *Biochemistry.* 2009;**48**(41):9848–57. doi: 10.1021/bi901126u. [PubMed: 19772300].
45. Sheng C, Ji H, Miao Z, Che X, Yao J, Wang W, et al. Homology modeling and molecular dynamics simulation of N-myristoyltransferase from protozoan parasites: active site characterization and insights into rational inhibitor design. *J Comput Aided Mol Des.* 2009;**23**(6):375–89. doi: 10.1007/s10822-009-9267-2. [PubMed: 19370313].
46. Macindoe G, Mavridis L, Venkatraman V, Devignes MD, Ritchie DW. HexServer: an FFT-based protein docking server powered by graphics processors. *Nucleic Acids Res.* 2010;**38**(Web Server issue):W445–9. doi: 10.1093/nar/gkq311. [PubMed: 20444869].
47. Dayer MR, Dayer MS, Ghayour O. Dynamic Behavior of Rat Phosphoenolpyruvate Carboxykinase Inhibitors: New Mechanism for Enzyme Inhibition. *The Protein Journal.* 2013;**32**(4):253–8. doi: 10.1007/s10930-013-9481-6.
48. Yang XG, Luo RY, Feng ZP. Using amino acid and peptide composition to predict membrane protein types. *Biochem Biophys Res Commun.* 2007;**353**(1):164–9. doi: 10.1016/j.bbrc.2006.12.004. [PubMed: 17174938].